the Σ^+-nucleon cross section is 45 mb and the K^+-nucleon cross section is 15 mb, and assuming each to travel one nuclear radius before emerging from the carbon nucleus.

The effect of Fermi momentum of the carbon proton was evaluated by assuming that 80 Mev/c of transverse momentum would lead to a clearly noncoplanar interaction, and that 100 Mev/c along the pion direction would lead to an apparent incident momentum that is clearly incorrect. Assuming the Gaussian distribution of proton momenta given by Cladis, Hess, and Moyer,[9] one then finds that a carbon event has only a 28% chance of not being rejected because of its proton motion.

[9] J. B. Cladis, W. N. Hess, and B. J. Moyer, Phys. Rev. 87, 425 (1952).

Multiplying these three attenuation factors by the ratio of carbon to hydrogen protons present in the propane, one obtains the figure of 11% contamination by spurious events from the carbon.

ACKNOWLEDGMENTS

We wish to thank the staff and crew of the Cosmotron Department, Brookhaven National Laboratory, for operating and making the Cosmotron available for this experiment, and Dr. Horace Taft, Dr. Charles Dechand, Dr. William Willis, Al Bachman, Frank Shively, and Al Howard for aid in operating the equipment. Dr. L. Mackey has assisted in analyzing the events. We are also indebted to the Cloud Chamber Group, Brookhaven National Laboratory, for assistance in preparing for the experiment.

PHYSICAL REVIEW VOLUME 118, NUMBER 2 APRIL 15, 1960

Small-Angle Proton Scattering at 3 Bev*

W. M. PRESTON, RICHARD WILSON, AND J. C. STREET
Cyclotron Laboratory, Harvard University, Cambridge, Massachusetts
(Received November 2, 1959)

The differential cross section for elastic scattering of 3-Bev protons has been measured with targets of hydrogen, carbon, copper, and lead over the angular range 0.5 to 4 degrees in the laboratory coordinate system. Within our limits of error, no evidence was found of Coulomb-nuclear interference with hydrogen, while with carbon there is indication of a real component of the nuclear scattering amplitude associated with a repulsive force. It is inferred from the extrapolated nuclear scattering cross section at zero degrees that appreciable scattering results form spin dependent forces with hydrogen but not with carbon. A derived value of the rms radius for p-p scattering exceeds that found in electron-proton scattering by a factor $\sqrt{2}$.

INTRODUCTION

THE purpose of this experiment was to measure directly the absolute values of some nuclear differential elastic-scattering cross sections $\sigma_e(\theta)$[1] for protons of 3-Bev energy, particularly at small angles where the Coulomb and nuclear elastic scattering are of comparable magnitude and the possibility exists of appreciable interference between the two. Since the Coulomb scattering amplitude is known, this gives information about the real and imaginary components of the nuclear scattering amplitude $f_n(\theta)$. At lower energies the effect is well known; for example, for 96-Mev protons on C and Al there is considerable destructive interference.[2] More generally, the differential cross sections at various energies furnish the data from which the parameters of any assumed nuclear potential must be calculated.

In the Bev energy range, the Coulomb and nuclear elastic scattering are of comparable magnitude at very small angles; these may be estimated crudely as follows. The point charge Coulomb scattering of protons at small angles θ in the laboratory system is given approximately by

$$\sigma_C(\theta)=4Z^2r_e^2(mc^2/pv)^2/\theta^4 \text{ cm}^2/\text{sr}, \quad (1)$$

where Z is the nuclear charge, $r_e=2.82\times10^{-13}$ cm, mc^2 is the electron self-energy, and p and v are the momentum and velocity of the incident proton in the laboratory system. The nuclear elastic scattering is mostly diffraction scattering resulting from absorption processes, principally meson production. Hence the forward scattering amplitude is approximately that due to a "black disk" of radius R cm:

$$\sigma_e(0)=\tfrac{1}{4}k^2R^4 \text{ cm}^2/\text{sr}, \quad (2)$$

where k is the propagation constant of the incident

* This research was supported by the Office of Naval Research and by the U. S. Atomic Energy Commission.

[1] We use the following notation for various cross sections: $\sigma_e(\theta)$ for the nuclear elastic differential scattering, $\sigma_C(\theta)$ for the Coulomb *point-charge* differential scattering, $\sigma(\theta)$ for the total effective elastic differential scattering, σ_e for the total nuclear elastic scattering, σ_a for the total nuclear absorption, and $\sigma_t=\sigma_e+\sigma_a$ for the total nuclear cross section.

[2] G. Gerstein, J. Niederer, and K. Strauch, Phys. Rev. 108, 427 (1957).

proton. At small angles the effect of a form factor will in any case be small. Equating $\sigma_c(\theta_E)=\sigma_e(0)$ and solving for the angle θ_E of equality, for protons of energy 3 Bev:

$$\theta_E=0.51Z^{\frac{1}{3}}/A^{\frac{1}{3}}R_0 \text{ degrees}, \quad (3)$$

where we have set $R=R_0A^{\frac{1}{3}}$ fermis, A being the atomic weight of the target nucleus. If we let $R_0=1$ for hydrogen and 1.25 for heavier nuclei, $\theta_E=0.51$, 0.44, 0.58, and 0.62 degree, respectively, for H, C, Cu, and Pb.

PREVIOUS WORK

There have been relatively few measurements of $\sigma(\theta)$ for Bev protons, due partially to the experimental difficulties in working at the required small angles. Smith, McReynolds, and Snow[3] used an internal CH_2 target in the Brookhaven Cosmotron proton beam, at energies from 0.44 to 1.0 Bev. They detected protons by counters at the angle required for elastic p-p collisions and thus were able to measure $\sigma(\theta)$ for hydrogen down to a minimum angle of 12°. Cork, Wenzel, and Causey[4] used a similar method at higher energies in the Berkeley Bevatron. By placing one of the counters inside the vacuum chamber, they were able to get to smaller angles, but not down to the interference region. They measured $\sigma(\theta)$ at energies and minimum angles of 2.24 Bev (5°), 4.40 Bev (3°), and 6.15 Bev (1.9°).

Batty and Goldsack[5] and Batty, Lock, and March[6] used a well collimated proton beam of 0.97-Bev energy from the Birmingham accelerator. The latter authors placed nuclear emulsions edgewise, one meter downstream from a carbon target, and counted fast proton track density as a function of scattering angle. They were able to separate protons coming from the target from a larger background coming from the collimator by the track angles in the emulsions. They could not separate out high-energy inelastic protons, but these were expected to amount to only a few percent. They measured $\sigma(\theta)$ for carbon from 5° down to $1\frac{1}{2}$°, well into the Coulomb region, and fitted their results with an optical model calculation. The central potential term seemed to require a small negative real part.

EXPERIMENTAL METHOD

General

At 3-Bev energy the scattering angles of interest have become so small that a narrow, well defined pencil beam of protons is required for adequate resolution. Inelastically scattered protons (those which have created mesons) are also peaked rather strongly forward in the laboratory system and may have lost a relatively small fraction of their energy; it is desirable to have sufficient energy resolution to separate them from the elastic scattering. Finally, there is always a background of high-energy particles coming from defining apertures and shields which must be eliminated.

Under these conditions, nuclear emulsions offer certain advantages over counters as detectors in addition to economizing machine operating time. They were used in the present experiment in conjunction with an analyzing magnetic field. Figure 1(a) shows schematically the principal features of the beam collimation and the target and magnet locations at the Brookhaven Cosmotron, which was the source of 3-Bev protons.

The so-called pencil beam issued from the vacuum chamber and passed through a $\frac{3}{4}$-in. diameter hole in a brass collimator block A, 18 in. thick. The beam was almost parallel in the horizontal plane and slightly diverging vertically. B was a 24-in. steel block whose face was $\frac{13}{16}$ in. from the beam axis; it threw a shadow such that protons from A could not hit any shielding on the right side (looking up stream) and be scattered into the photographic plates at P. The beam next passed through the strong-focusing quadrupole pair SF and a bending magnet No. 1 which was used (at very low field) to trim the beam position in the horizontal plane. The hole in the main shield was enlarged on the right side so that the wall was shadowed by B. On the left was a 48-in. thick steel collimator block C with a $\frac{1}{8}$-in. lip 24 in. long. The target T was 15 in. from C; 94 in. beyond, the beam and scattered particles from T entered the vertical field of Magnet No. 2.

Figure 1(b) shows the target region on an enlarged scale. Magnet No. 2 had a 4-in. gap and poles 18 in. ×36 in. It was aligned so that the beam passed parallel to the 36-in. edge and 4 in. from it. A light-tight plate holder was built to fit in an accurately reproducible

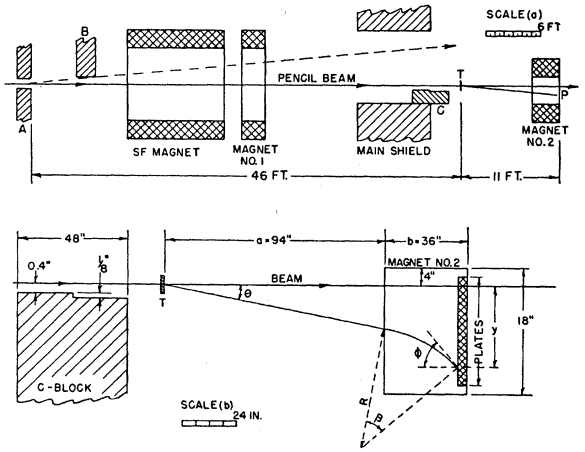

FIG. 1. Experimental arrangement. (a) The pencil proton beam, collimators, and analyzing magnet. (b) The target region on an enlarged scale. A proton scattered at the angle θ is bent by Magnet No. 2 so as to be incident on the plates at an angle φ. Note: the vertical scale is enormously exaggerated.

[3] L. W. Smith, A. W. McReynolds, and G. Snow, Phys. Rev. **97**, 1186 (1955).
[4] B. Cork, W. A. Wenzel, and C. W. Causey, Jr., Phys. Rev. **107**, 859 (1957).
[5] C. J. Batty and S. J. Goldsack, Proc. Phys. Soc. (London) **A70**, 165 (1957).
[6] C. J. Batty, W. O. Lock, and P. V. March, Proc. Phys. Soc. (London) **73**, 100 (1959).

position along the rear of the gap. It held 4 Ilford 2-in. ×3-in. nuclear plates with 200-micron emulsions inclined at exactly 5° to the horizontal (see Fig. 2). A proton scattered at an angle θ, Fig. 1(b), is bent through an additional angle β, inversely proportional to its momentum, by the magnetic field H of magnet No. 2. It strikes the inclined nuclear plates (in the median plane of the magnet) at an azimuth angle $\varphi=\theta+\beta$ relative to the beam and at a distance y from the beam axis. From the geometry,

$$b=R(\sin\varphi-\sin\theta), \tag{4}$$

$$y=a\tan\theta+R(\cos\theta-\cos\varphi), \tag{5}$$

where a and b are, respectively, the distances from the target to the effective edge of the magnetic field, and from the field edge to the plates, measured along the beam axis. In scanning the plates, the impact angle φ and distance from the axis y are measured for each track; knowing a and b we can then compute the scattering angle θ and the radius of curvature R, and from R and the magnetic field H, the momentum p of elementary particles of known mass, assumed to have come from the target. From the surface density of tracks and the inclination angle of the plates we compute the scattered flux normal to the beam, as a function of θ.

The plate holder was adjusted laterally (parallel to the back face of the magnet) so that the deflected pencil beam just missed the edge of the first of the 4 inclined plates, which were accurately located by pins. The beam itself passed normally through a fifth plate, oriented vertically in the back of the holder to minimize scattering, so that a record was obtained of the exact average beam position during each run.

The axis and cross section of the pencil beam were found by exposing x-ray films at various positions. The beam cross section at the down stream face of B, Fig. 1(a), was 2 in. high by $\frac{3}{4}$ in. wide. The SF magnet

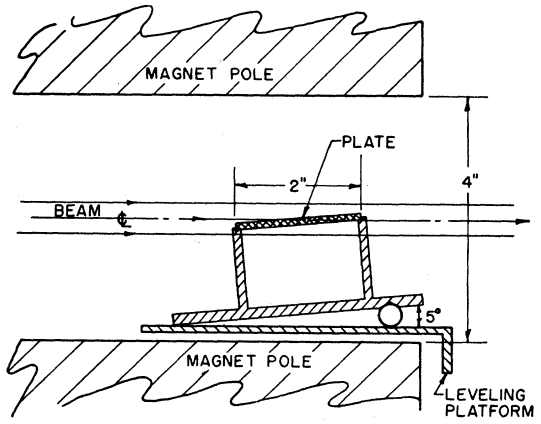

FIG. 2. The plate holder (schematic) shown in position between the poles of the analyzing magnet. Not shown is the light-tight cover which fits over the plate holder.

was adjusted to give the best focus at the plate position P. Scattering along the path was very greatly reduced by putting in two long, sausage-shaped polyethylene gas bags. One extended from the target upstream about 35 feet and for reasons of safety was filled with helium; the block C was inside of this bag. The other, filled with hydrogen, extended from the target to the plate holder. Most of the beam at the plates fell within an ellipse with horizontal and vertical axes of 10 and 15 mm, respectively.

Solid targets of carbon, copper, or lead were 1 in. wide and held in a frame which had been accurately located on the axis. The liquid hydrogen target was a thin copper box, $15\frac{5}{8}$ in. in length along the beam and 15 in. deep, insulated by Styrafoam, and having in all 12 thin Mylar windows with a free aperture of 6 in. and a total thickness of 0.025 g/cm^2.

Beam Monitoring

Our cross sections are based on the measurements at Brookhaven, with the same proton pencil beam, of the $C^{12}(p,pn)C^{11}$ cross section by Cumming, Friedlander, and Swartz.[7] Their method made use of a cylinder of scintillator plastic, an inch or more in diameter and one inch thick, exposed in the pencil beam at reduced intensity so that the absolute number of protons per pulse could be counted with a conventional scintillation telescope. The induced C^{11} activity was determined after the run in a low-level, high-efficiency counter developed for the purpose.[8] Following calibration, the activation of similar plastic cylinders can be used as an absolute monitor at much higher intensities for which direct counting in the beam becomes impossible.

In the present experiment, we employed a fast Čerenkov counter with an 8-inch aperture,[9] located in the proton beam after it had passed through the analyzing magnet and subtending at the target a half-angle of about 1.4 degrees. In a separate five-minute cosmotron run, this was calibrated against a 3-in. diameter, one-inch thick cylinder of scintillator plastic placed in the beam in front of the Čerenkov counter and later counted for C^{11} activity.[10] The number of protons incident was thus determined to be 2.48×10^9, using a $C^{12}(p,pn)C^{11}$ cross section at 3.0 Bev of 29.2 mb, which includes an allowance for secondary particles produced in the thick plastic cylinder. The uncertainty in this cross section was estimated to be $\pm5\%$.[7]

During plate exposures, the output of an argon-filled ionization chamber was fed to an Esterline-Angus recorder[11] and furnished a permanent record of pulse-

[7] J. B. Cumming, G. Friedlander, and C. E. Swartz, Phys. Rev. **111**, 1386 (1958).
[8] J. B. Cumming and R. Hoffman, Brookhaven National Laboratory Report BNL-3775 (unpublished).
[9] This counter was developed at Brookhaven by Dr. C. E. Swartz, who very kindly loaned it to us.
[10] We are indebted to Dr. Cumming for measuring this activity and for much helpful advice.
[11] Dr. J. Kopp designed this monitor and operated it for us.

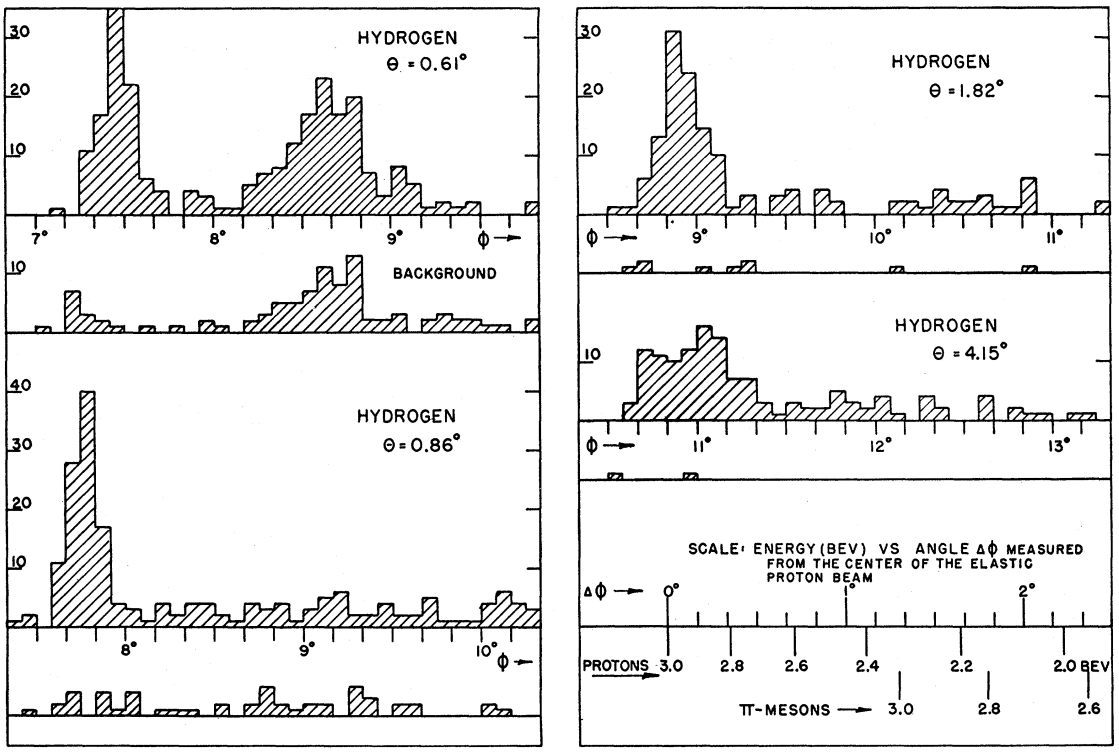

FIG. 3. Histograms of the number of minimum ionizing tracks, in angular intervals $\Delta\varphi = 5$ minutes, vs φ, the angle of incidence on the plate. Four examples are shown, for a liquid hydrogen target at different scattering angles θ. The background (empty liquid hydrogen container) is shown on the same scale. In the lower right is an energy scale for protons and π mesons, in degrees of φ measured from the center of the elastically scattered peak.

by-pulse variations in beam intensity as well as a check on the operation of the Čerenkov counter.

Small corrections to the readings of the Čerenkov counter were required because of nuclear absorption and scattering in the targets; they totalled about 3% for the hydrogen and carbon targets and less than one percent for the others. Single and multiple Coulomb scattering corrections were negligible.

Scanning

The 2-in.×3-in., 200-micron Ilford G5 plates were processed at low temperature (4°C) in order to minimize distortions in the emulsion. They were examined with microscopes having precision stages designed for multiple Coulomb scattering measurements. The scanning was done in strips approximately parallel to the direction of incidence of elastically scattered protons defined by the angle φ of Fig. 1(b). Minimum ionizing tracks were located by scanning in depth and were traced back to their point of entry into the emulsion. If this point lay within the limits of the strip, the coordinates of 3 points at 500-micron intervals along the track were measured with a micrometer eyepiece. Relative values of the incidence angle φ for each track could thus be measured with an accuracy better than ± 0.1 degree; the uncertainty in the absolute values was somewhat larger due to errors in the positioning of the plates in the plate holder, beam alignment, etc. Tracks whose dip angle in the emulsion lay outside acceptable limits were rejected, although these were uncommon.

Selected areas at intervals along the center line of the plates [in the direction y, Fig. 1(b)] were scanned in order to measure the track density as a function of scattering angle θ. The area required to obtain 100 tracks of elastically scattered protons never amounted to more than 10 mm².

EXPERIMENTAL RESULTS

Three sets of exposures were made at the Brookhaven cosmotron. The first was in the nature of a trial to determine exposures and feasibility. The second resulted in satisfactory plates for C and Cu targets; the hydrogen exposures had a large unexplained background and our beam monitor failed to function. While waiting for another run, the C and Cu plates were scanned and values of *relative* differential cross sections obtained. A third run was almost completely successful, with targets of H, C, Cu, and Pb. The plates for C and Cu were scanned at 3 scattering angles and these absolute cross sections used to normalize the more extended results obtained previously.

Hydrogen

The target contained 2.82 g/cm² of liquid hydrogen (density 0.071 g/cm³). Figure 3 shows histograms, at several values of the scattering angle θ, of the number of minimum ionizing tracks per 5 minute interval in φ vs φ, the angle of incidence on the plate. The latter, from Eq. (1), is related to the momentum p of a charged particle by $\varphi=\theta+A/p$ for small angles, where A is a constant. The relation between φ and the kinetic energy of protons and π mesons is shown by the scale at the lower right of Fig. 3.

The peak corresponding to elastically scattered protons is readily apparent. At small scattering angles, about half the tracks fall within an angular interval $\Delta\varphi=10$ minutes, corresponding to $\Delta E=100$ Mev for 3-Bev protons. The greater width of the elastic peak at $\theta=4.15°$ is due to the angle subtended off-axis by the 40 cm length of the liquid hydrogen target.

The background from the empty hydrogen target is also shown in Fig. 3. It amounts to a maximum of about 15%, within the angular limits which comprise the elastic peak, at small scattering angles. It becomes almost negligible at larger angles.

Tracks at angles greater than those within the elastic peak correspond to protons of energy less than 3.0 Bev. The large peak in the histogram for $\theta=0.61°$, centered at $\varphi=8°40'$, is of spurious origin.[12] For $\theta>1°$, most of these lower energy protons result from inelastic processes in hydrogen, as is shown by their absence in the background exposure. A forward-directed proton which has produced one π meson has a maximum energy of about 2.85 Bev. In the histogram for $\theta=1.82°$ of Fig. 3, tracks having values of φ from 9°20′ to 11° correspond roughly to proton energies of 2.8 to 2.0 Bev. The separation of elastic and inelastic scatterings is thus nearly complete except at the largest scattering angles.

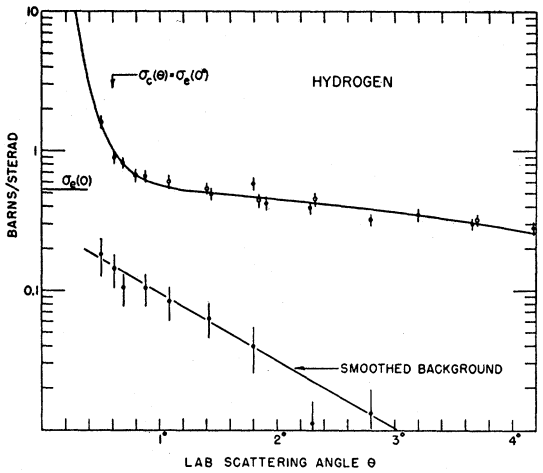

FIG. 4. The differential cross section $\sigma_e(\theta)$ for elastic proton-proton scattering at 3 Bev, from the present experiment. Solid and open points represent data from two independent runs. The solid curve is a plot of Eq. (6) with a forward scattering amplitude $\sigma_e(0)=0.54$ barn/sr and a Gaussian form factor with radial parameter. $a=0.86$ fermi.

The differential scattering cross sections $\sigma(\theta)$ for hydrogen computed from our data are listed in Table I(a) and plotted in Fig. 4. Results from two

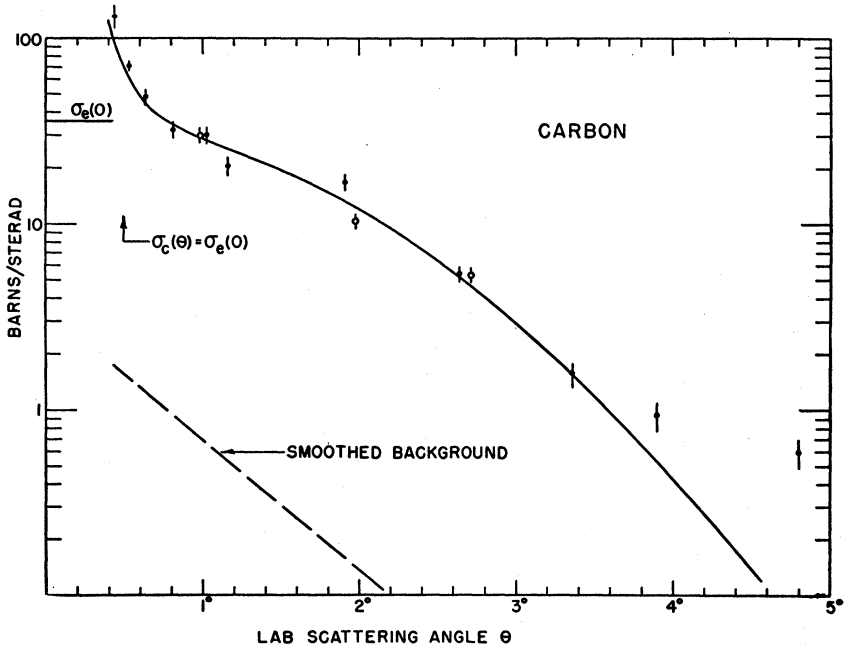

FIG. 5. Differential cross sections for carbon. The circled points were absolute measurements, to which the remaining points were normalized. The smooth curve is drawn from Eq. (6) using $\sigma_e=35.9$ barns/sr and a Gaussian form factor with the parameter $a=2.2$ fermis.

[12] It is due to 3.0-Bev protons from the fringes of the pencil beam which have passed through the 24-in. thick "lip" of the collimator [block C in Fig. 1(b)] and have thereby lost about 700-Mev energy. At angles $\theta>1°$ these protons are effectively cut off by the remainder of the collimator.

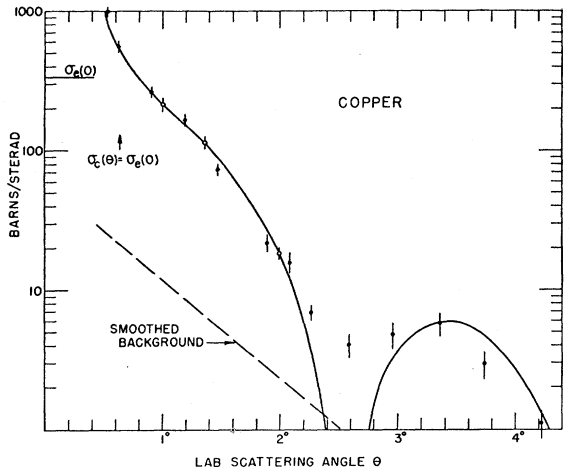

FIG. 6. The differential cross section for copper. The circled points were absolute measurements to which the remaining points were normalized. The smooth curve is drawn from Eq. (6) using $\sigma_e(0)=335$ barns/sr and a Bessel function form factor $F=2J_1(x)/x$, with $x=kR\theta$, $R=4.43$ fermis.

separate runs, Exposures No. 3 and No. 3A, are in good agreement.

Carbon

The target contained 4.70 g/cm² of carbon. The data are given in Table I(b) and plotted in Fig. 5. The three points of Exposure No. 5 (open circles in Fig. 5) are absolute cross sections based on the third run. The remaining points represent relative cross sections from the second run, normalized to a curve determined by the 3 absolute values.[13]

Copper and Lead

The thickness of the copper target was 1.44 g/cm² and that of the lead 0.602 g/cm². The cross sections are given in Table I(c) and I(d) and plotted in Figs. 6 and 7. As in the case of carbon, relative cross sections for copper obtained in an early run were normalized to the absolute values at 3 angles obtained in the third experiment. All the data for lead represent absolute measurements. The circled and uncircled points in Fig. 7 represent data from two different exposures, No. 8 and No. 7, respectively, the former 8.2 times as intense as the latter in order to get a higher track density at large scattering angles. The disagreement at the two angles measured on both exposures is unexplained; it is probably due to systematic scanning error.[14]

[13] The actual normalization was most accurately accomplished by a method described in the following section.

[14] This set of plates was extremely difficult to scan because of the relatively high background. In order to keep multiple scattering the same in targets of carbon and lead, the number of atoms of lead/cm² must be about 0.7% of the number of carbon atoms.

DERIVATION OF PARAMETERS

We derive from these data three parameters of consequence: the forward nuclear elastic scattering cross section, $\sigma_e(0)$; the magnitude of the real part of the scattering amplitude f_r, and the root-mean-square radius of interaction, r_m. The method follows Bethe.[15] It is assumed that the same form factor $F(k\theta)$ describes the angular distribution of both nuclear and Coulomb scattering. Here $k\theta$ is the (invariant) momentum transfer, k the propagation constant and θ the scattering angle, both in the laboratory system. If the experimental cross sections are divided by the proper $F^2(k\theta)$, they will describe the scattering from a point nucleus.[16] Thus in the simplest case, when there is no interference between nuclear and Coulomb scattering, we may write

$$\sigma(\theta)=[\sigma_e(0)+\sigma_c(\theta)]F^2(k\theta). \tag{6}$$

For values of the form factor which are not too small, a Gaussian approximation will be convenient and sufficiently accurate,

$$F(k\theta)=e^{-ka\theta/\sqrt{2}}, \tag{7}$$

as given by Eq. (7). The radial parameter a is related to the rms radius r_m by Eq. (8).

$$r_m=(\tfrac{3}{2})^{\frac{1}{2}}a. \tag{8}$$

If Eqs. (6) and (7) were exactly true, a plot of the function

$$y=[\sigma(\theta)/F^2(k\theta)]-\sigma_c(\theta) \tag{9}$$

would show a constant value, independent of θ and numerically equal to $\sigma_e(0)$.

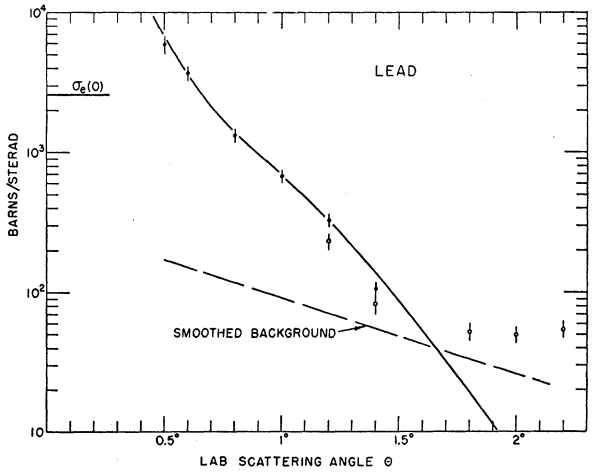

FIG. 7. The differential cross section for lead. The smooth curve is drawn for Eq. (6) using $\sigma_e(0)=2600$ barns/sr and a Gaussian form factor, parameter $a=5.15$ fermis.

[15] H. A. Bethe, Ann. Phys. 3, 190 (1958).

[16] Strictly speaking, this is only true in Born approximation. However, it has been shown by many authors that the effects of multiple scattering, provided they are not too large, depress the cross section independently of θ, for small values of θ.

Hydrogen

In Fig. 8(a) we have plotted the values of $\sigma(\theta)$ for hydrogen, taken from Table I, after dividing by $F^2(k\theta)$ from Eq. (7) and subtracting $\sigma_c(\theta)$ from Eq. (1). We have tried to adjust the parameter a so that the points lie on a horizontal line, $y=$const. The line drawn is a least-squares fit. The datum points, each based on 100 measured tracks and having therefore (except for the two at smallest angles) a statistical standard deviation of 10%, have together an rms deviation from the straight line of about the same magnitude and show no obvious trend. We may make three observations:

(a) The value found for the radius parameter $a=0.86$ (in fermi units, 10^{-13} cm) is determined principally by the 4 experimental points at $\theta\geqslant 3.2°$; it would have been desirable to have had data at wider angles. The *process of adjustment* is sufficiently objective so that values of a differing by $\pm 10\%$ from that given above can be excluded as most unlikely; the standard deviation from this cause may be half as great. No further uncertainty is introduced by error in the absolute cross section. However, a is subject to any (unknown) systematic errors in the cross-section measurements which are a function of the scattering angle.

(b) The value $\sigma_e(0)=0.54$ barn/sr found for the forward scattering cross section is virtually independent of the value chosen for a. We can assign to it a statistical standard deviation of $\pm 3\%$, to which must be added the uncertainty in the monitor calibration of at least 5%, giving a total of about $\pm 6\%$. This contains no allowance for systematic errors.

TABLE I. Experimental differential elastic scattering cross sections $\sigma(\theta)$ in barns/sr at the laboratory scattering angle θ degrees. The errors given are statistical standard deviations based only on the number of tracks counted. The cross sections of Exp. No. E-8 have been normalized to the absolute measurements of Exp. No. 5, those of Exp. No. E-9 to the absolute values of Exp. No. 6.

Exp. No.	θ	$\sigma(\theta)$	Exp. No.	θ	$\sigma(\theta)$
		(a) Hydrogen			
3	0.50	1.60±0.18	3	2.80	0.32±0.03
3	0.61	0.89±0.10	3	3.20	0.35±0.04
3	0.68	0.82±0.10	3	3.68	0.30±0.03
3	0.88	0.66±0.08	3	4.18	0.28±0.03
3	1.08	0.61±0.07	3A	0.79	0.66±0.08
3	1.42	0.49±0.06	3A	1.40	0.53±0.06
3	1.82	0.58±0.06	3A	1.82	0.44±0.05
3	1.91	0.42±0.05	3A	2.30	0.45±0.05
3	2.30	0.39±0.04	3A	3.68	0.32±0.03
		(b) Carbon			
E-8	0.44	130±14	E-8	2.64	5.35±0.58
E-8	0.53	71±5.3	E-8	3.36	1.54±0.25
E-8	0.63	48±5.3	E-8	3.90	0.93±0.17
E-8	0.81	32±3.6	E-8	4.80	0.59±0.10
E-8	1.00	30±3.3	5	0.99	30.0±3.0
E-8	1.16	20.5±2.2	5	1.98	10.3±1.0
E-8	1.91	16.8±1.8	5	2.72	5.3±0.53
		(c) Copper			
E-9	0.53	995±105	E-9	2.59	4.0±0.9
E-9	0.62	560±59	E-9	2.96	4.7±1.1
E-9	0.90	266±28	E-9	3.36	5.7±1.2
E-9	1.19	166±18	E-9	3.74	2.9±0.7
E-9	1.47	73±8	E-9	4.12	1.1±0.28
E-9	1.89	21.7±3.2	6	1.00	215±23
E-9	2.08	15.8±3.0	6	1.36	115±12
E-9	2.27	6.9±1.0	6	1.99	18.2±2.2
		(d) Lead			
7	0.50	5800±800	8	1.20	230±30
7	0.60	3660±380	8	1.40	82±14
7	0.80	1300±140	8	1.80	52±8
7	1.00	670±75	8	1.98	49±7
7	1.20	320±39	8	2.20	54±7
7	1.40	103±16			

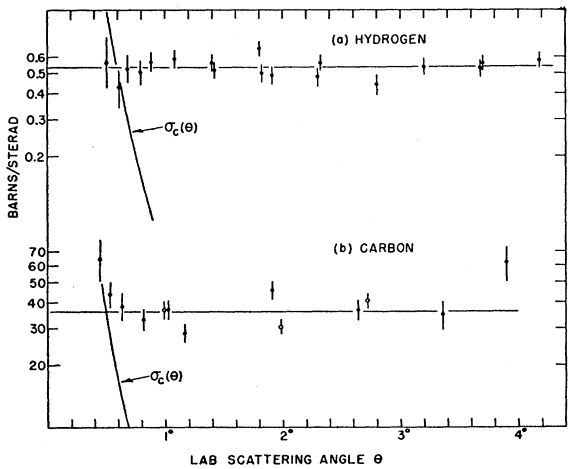

FIG. 8. Differential cross sections for (a) hydrogen and (b) carbon after dividing by a Gaussian form factor and then subtracting the calculated Coulomb cross section, $\sigma_C(\theta)$.

Carbon

For carbon, as in the treatment of the hydrogen data, the parameter a of a Gaussian form factor was adjusted to remove the angular dependence of the scattering cross sections. First a was determined from the 3 absolute cross sections, Exposure No. 5 of Table 1(b). The results are plotted as open circles in Fig. 8(b). The remaining (relative) cross sections were all multiplied by a suitable normalizing constant so that, after dividing by the already-determined form factor and subtracting the calculated $\sigma_c(\theta)$, they lay on the best horizontal line through the absolute points.

(a) The value found above, $a=2.2$ fermis, is probably uncertain to $\pm 10\%$ considering the arbitrariness in its derivation from the primary data. At $\theta=3.36°$ the form factor is already small: $F^2=0.044$. It is not surprising that the Gaussian function should fail at still larger angles and such points were ignored in adjusting a.

(b) The value $\sigma_e(0)=36$ barns/sr is principally determined by the single absolute datum point at 1°; it should be given a *statistical* standard deviation slightly greater than 10%. (But see below, Note added in proof.)

Copper

The copper data were treated similarly to those of carbon and the results are shown in Fig. 9(a). Since

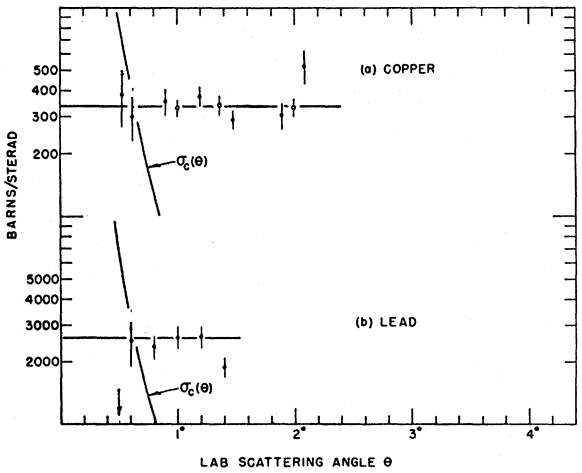

FIG. 9. Differential cross sections for (a) copper and (b) lead, after dividing by an adjusted form factor (see text) and subtracting the calculated Coulomb scattering.

there is evidence (Fig. 6) of a secondary scattering peak at about the position expected from a "black disk" diffraction formula, we tried in this case a form factor $F(k\theta)=2J_1(x)/x$, where $x=kR\theta$ and $J_1(x)$ is a first order Bessel function, instead of a Gaussian. The radius parameter R was adjusted for the 3 circled points in Fig. 9(a), derived from absolute cross sections, and then used for the relative data after normalization.

(a) With $R=4.43$ fermis, the three absolute points lie in a better-than-should-be-expected fashion on a horizontal line. At $\theta=2°$, the form factor $F^2=0.05$; it naturally fails beyond. However, a Gaussian with $a=3.7$ fermis gives almost equally good results. The statistical uncertainty appears to be somewhat less than in the case of carbon.

(b) The Bessel function form factor of Fig. 9(a) gives $\sigma_e(0)=335$ barns/sr, the Gaussian $\sigma_e(0)=430$ barns/sr. This considerable difference must engender caution. In the case of hydrogen, any reasonable form factor is nearly unity at the measured small-angle points which largely determine $\sigma_e(0)$. For a heavy nucleus like copper, however, this is not so. If the experimental point at 2° is used to adjust the radius parameter, there is a substantial difference between the Bessel and Gaussian functions at 1°.

Lead

The lead cross sections from Table I(d) Exposure 7, are plotted in Fig. 9(b) after division by an adjusted Gaussian form factor and subtracting the Coulomb term.

(a) The value obtained for the radial parameter is $a=5.15$ fermis. Values of a 10% higher or lower give noticeably poorer fits.

(b) From Fig. 9(b), $\sigma_e(0)=2600$ barns/sr. This, however, is very sensitive to the value chosen for a; the uncertainty is at least ± 500 barns/sr.

DISCUSSION

Coulomb Interference

Following Bethe's treatment, as applied by him to the scattering of 310-Mev protons from carbon,[15] we write for the differential cross section for unpolarized elastic scattering from a point nucleus:

$$\sigma(\theta)/F^2(\theta)=|\bar{g}_C+\bar{g}_n|^2=|g_C+(g_{nR}+ig_{nI})e^{2i\eta}|^2$$
$$=g_C^2+g_{nI}^2+g_{nR}^2+2g_C(g_{nI}\sin 2\eta+g_{nR}\cos 2\eta), \quad (10)$$

where $\bar{g}_C$ and $\bar{g}_n$ are the complex Coulomb and spin-independent nuclear scattering amplitudes, respectively; g_C, g_{nR}, and g_{nI} are real quantities which are taken as positive for attractive central potentials, and 2η is the average difference between the Coulomb phase shifts applicable to the Coulomb and nuclear scattering. Both interference terms are destructive as long as the real nuclear central potential is attractive, i.e., $g_R>0$.

Bethe gives a method for averaging the phase-shift difference over the nuclear volume and derives:

$$\eta=[Ze^2/\hbar v]\ln(\theta_0/\theta), \quad (11)$$

which goes to zero at the angle θ_0 given by

$$\theta_0=1.06/ka \text{ radians}, \quad (12)$$

where a is the radial parameter of the (assumed) Gaussian distribution of the nuclear potential.

For 310-Mev protons on carbon, Bethe found that $g_{nR}\ll g_{nI}$. On the assumption that this is still true at 3 Bev, we have tried to estimate the various terms in Eq. (10), with the results shown in Table II. We have

TABLE II. Calculated values of the terms in Eq. (10). The radius parameter a is in fermis, the scattering angle θ in degrees, the phase difference 2η in radians. The numbers in the last four columns are cross sections in barns/sr. The negative sign is by convention associated with a repulsive force, in this case g_C.

a	θ	2η	g_{nI}^2	g_C^2	$2g_Cg_{nI}\sin 2\eta$	$2g_Cg_{nR}\cos 2\eta$
			Hydrogen			
0.86	0.50	0.030	0.54	1.04	−0.045	$-2.04\,g_{nR}$
0.86	0.61	0.027	0.54	0.47	−0.028	$-1.37\,g_{nR}$
0.86	0.68	0.026	0.54	0.30	−0.021	$-1.09\,g_{nR}$
0.86	0.79	0.024	0.54	0.167	−0.014	$-0.82\,g_{nR}$
0.86	0.88	0.022	0.54	0.108	−0.011	$-0.66\,g_{nR}$
0.86	1.08	0.019	0.54	0.047	−0.006	$-0.43\,g_{nR}$
			Carbon			
2.20	0.44	0.106	36	62.3	−10.0	$-15.8\,g_{nR}$
2.20	0.53	0.090	36	29.7	− 6.0	$-10.9\,g_{nR}$
2.20	0.63	0.074	36	15.3	− 3.4	$-7.8\,g_{nR}$
2.20	0.81	0.050	36	5.3	− 1.4	$-2.3\,g_{nR}$
2.20	1.00	0.032	36	2.4	− 0.6	$-1.55\,g_{nR}$
			Copper			
3.70	0.53	0.204	337	688	−196	$-52\,g_{nR}$
3.70	0.62	0.133	337	367	− 93	$-38\,g_{nR}$
3.70	0.90	0	337	83	− 0	$-18\,g_{nR}$
			Lead			
5.15	0.50	0.24	2600	7070	−2060	$-168\,g_{nR}$
5.15	0.60	0.025	2600	3360	− 148	$-116\,g_{nR}$
5.15	1.00	0.0	2600	435	− 0	$-42\,g_{nR}$

used our experimental values of a in Eqs. (11) and (12) to calculate the phase difference angle 2η. In the absence of interference, or in any case at larger angles where the calculated value of $\sigma_C(\theta)=g_C^2$ is small, the quantity $y=\sigma(\theta)/F^2(\theta)-\sigma_C(\theta)\approx g_{nI}^2$. We can then estimate the two interference terms, the first of which occurs even if the nuclear scattering amplitude is purely imaginary, the second only if it has a real component. Interference should show up in the plots of Figs. 8 and 9 by departure of the plotted points at small angles from the line $y=$const.

In the case of hydrogen, the predicted values in Table II of the "imaginary" interference term are too small to show up in Fig. 8(a), due to the statistical errors in our data. However, we can probably exclude the presence of a "real" term of a magnitude given by a value of $g_{nR}\geqslant 0.1 g_{nI}$. (This conclusion does not depend on an accurate evaluation of the phase shift, as long as the latter remains small.)

With carbon, Fig. 8(b), the small angle points appear to be significantly high. The predicted "imaginary" interference term in Table II would lower the cross section; an increase would result from the second interference term if g_{nR} were negative, indicating the presence of a *repulsive* nuclear potential.[16a]

For copper, Fig. 9(a), there is no indication of interference. Table II predicts a lowering of the cross section at 0.53° of nearly 200 barns/sr due to the first interference term. In the case of lead, Fig. 9(b), the calculated value of y for the point at 0.50° (not shown, because it is off scale) is 600±1600 barns/sr. While not inconsistent with the large destructive interference predicted in Table II, this result is not significant because of the large statistical error.

At angles for which $\sigma_C(\theta)\geqslant\sigma_e(0)$, the relative statistical error in $y=[\sigma(\theta)/F^2]-\sigma_C(\theta)$ becomes unmanageably great. For heavier elements, the form factor F introduces further uncertainty. Even were our experimental accuracy considerably increased, an analysis of the type we have attempted is clearly inadequate to determine independently so many parameters.

TABLE III. Calculated values of: (1) $r_m=(3/2)^{\frac{1}{2}}a$ fermis, the rms nuclear radius calculated from values of the parameter a derived in the present experiment. The value for copper, in parentheses, is a "black disk" radius. (2) r_e is the rms nuclear radius derived from electron scattering experiments. (3) $\sigma_e(0)$ is the nuclear elastic forward scattering cross section, in barns/sr, derived from the present experiment. (4) The values of $[(k/4\pi)\sigma_t]^2$, in barns/sr, are calculated from interpolated values of the total cross section taken from Figs. 10 and 11.

Element	r_m	r_e	$\sigma_e(0)$	$[(k/4\pi)\sigma_t]^2$	Form factor
H	1.05	0.77[a]	0.54	0.44	Gaussian
C	2.7	2.4[b]	36	33	Gaussian
Cu	4.5	4.06[c]	430	360	Gaussian
Cu	(4.43)	4.06[c]	335	360	Black disk
Pb	6.3	5.42[c]	2600	1750	Gaussian

[a] E. E. Chambers and R. Hofstadter, Phys. Rev. **103**, 1454 (1956).
[b] H. F. Ehrenberg et al., Phys. Rev. **113**, 666 (1959).
[c] R. Hofstadter, *Annual Review of Nuclear Science* (Annual Reviews, Inc., Palo Alto, 1959), Vol. 7, p. 231.

[16a] *Note added in proof.*—This conclusion has been confirmed by recent data; we have measured absolute cross sections for carbon at eight additional angles down to 0.45°. Disregarding the data of Exp. E-8, Table I, which were not absolute, the results can be described by Eq. (10) with $\eta=0$, $g_{nI}^2=30$ barns, $g_{nR}^2=3$ barns, $\sigma_e(0°)=33$ barns. Thus $|g_{nR}|=0.3|g_{nI}|$ and has the same sign as g_C.

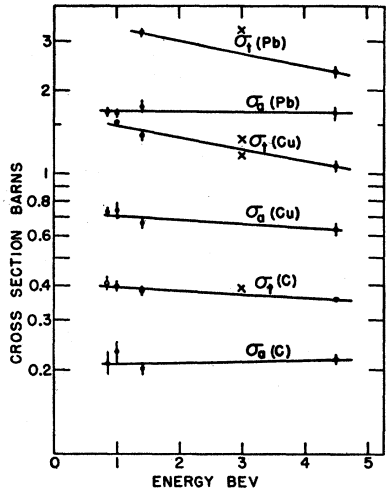

FIG. 10. Total cross sections: C, Cu, and Pb. At 0.86 Bev: F. F. Chen, C. P. Leavitt, and A. M. Shapiro, Phys. Rev. **103**, 211 (1956), σ_t and σ_a for protons. At 0.99 Bev: N. E. Booth, B. Ledley, D. Walker, and D. H. White, Proc. Phys. Soc. (London) **A70**, 209 (1957), σ_a and σ_t for protons. At 1.4 Bev: T. Coor, D. A. Hill, W. F. Hornyak, L. W. Smith, and G. Snow, Phys. Rev. **98**, 1369 (1955) σ_t and σ_a for neutrons. At 4.5 Bev: J. H. Atkinson, W. N. Hess, V. Perez-Mendez, R. W. Wallace. σ_t and σ_a for neutrons. The crosses at 3.0 Bev are the values of σ_t computed from the relation $\sigma_t=(4\pi/k)[\sigma_e(0^0)]^{\frac{1}{2}}$ using values of the forward scattering amplitude $\sigma_e(0)$ from the present experiment.

Forward Scattering Cross Section

In Table III we have compared our values of $\sigma_e(0)$, the nuclear forward scattering cross section, with calculated values of $[(k/4\pi)\sigma_t]^2$. From the optical theorem, these should be equal if $\sigma(0°)=g_{nI}^2$, i.e., if the nuclear scattering amplitude is purely imaginary. We have used for σ_t values interpolated between recent total cross-section measurements. For hydrogen we interpolate from the results of Longo *et al.*[17] a $\sigma_t=42.9\pm0.5$ mb. For C, Cu, and Pb we use interpolated values from Fig. 10.

In the case of hydrogen, $\sigma_e(0)-[(k/4\pi)\sigma_t]^2=0.10\pm0.05$ barn/sr, if we take $\sigma_t=0.043$ barn. Since we have shown it unlikely that $g_{nR}^2\geqslant 0.01 g_{nI}^2$, the explanation for this cannot be the existence of a sizeable real term in the scattering amplitude. The principal uncertainty in our result is the monitor calibration based on the $C^{11}(p,pn)$ cross section; the good agreement for carbon shown in Table III between $\sigma_e(0)$ and $[(k/4\pi)\sigma_t]^2$ gives confidence in the values we have used. The difference would disappear if σ_t has the value 0.048 barn at

[17] M. J. Longo, J. A. Helland, W. N. Hess, B. J. Moyer, and V. Perez-Mendez, Phys. Rev. Letters **3**, 568 (1959).

3 Bev, but this is well above direct measurements. These considerations indicate that the excess scattering arises from a term, neglected in Eq. (10), which is present in p-p scattering but absent in the scattering from nuclei. It may come from a spin-dependent force.

In a recent measurement of p-p scattering at 8.5 Bev in emulsions,[18] the forward cross section was found to be at least twice that predicted from a purely imaginary central potential. However, no measurements were attempted in the region of Coulomb interference so that a real term cannot be excluded at this energy.

As stated above, for carbon $\sigma_e(0)$ equals $[(k/4\pi)\sigma_t]^2$ within our limits of accuracy. For copper and lead, the choice of form factor introduces an additional error into our determination of $\sigma_e(0)$ and the disagreement is not significant.

Nuclear Radius

In Table III we compare the rms nuclear radius r_m deduced from our data with the corresponding quantity r_e found in electron-nuclear scattering. For hydrogen, the value $r_e=0.77\pm0.05$ fermi is widely interpreted as being the radius of a pion cloud surrounding a "bare" proton.

Pion proton scattering has been analyzed by Blohincev, Barašenkov and Grišin,[19] who find a root-mean-square radius $0.82\pm0.06\times10^{-13}$ cm. It is tempting to assume that the pion proton interaction proceeds entirely by a strong short range pion-pion interaction, which would give automatic agreement between the pion scattering and the electron scattering radii.

Other p-p scattering data, in the Bev energy region and at wider angles, have been analyzed by Cork, Wenzel, and Causey.[4] The results at wide angles are of course model dependent and it is not possible to obtain a unique value for the rms radius. Their various models gave proton radii ranging from 0.9 to 1.0 fermi, all larger than the electron scattering value. If one again envisages a strong pion-pion interaction, the nucleon-nucleon interaction radius becomes $\sqrt{2}$ times the radius of the individual pion clouds, or about 1.09 ± 0.07 fermis, in agreement with our value of r_m. Nucleon-nucleon and pion-nucleon scattering data have recently been reviewed by Veksler[20] who comes to similar conclusions.

For other nuclei, we expect that the mean-square radius for proton scattering should be increased by about (0.77 fermi)^2 over the electron scattering value. For carbon this predicts an rms radius of 2.5 fermis; our value in Table III is somewhat larger. Perhaps some opacity effect already enters, rendering the approximation inadequate for heavy nuclei. The difference is increasingly evident in the comparison of r_m and r_e for copper and lead.

ACKNOWLEDGMENTS

The authors wish to express their appreciation to Dr. George B. Collins, Director of the Cosmotron Department, and to his staff for making this experiment possible and for aiding us in every way. Dr. Anatole Shapiro, Dr. Lee Young, and Dr. Joshua Kopp helped us generously during the Cosmotron exposures. Dr. Mildred Widgoff superintended the emulsion development and advised us in the scanning of the plates. The scanning was performed by Gladys Johnson, K. T. Mahanthappa, W. Martin, E. Constantinides, and K. Bowker.

[18] Chen Pu-in, V. B. Lubimov, P. K. Markov, M. G. Shafranova, and E. N. Tzganov, Document No. P-339, Joint Institute for Nuclear Research, Dubna, 1959 (unpublished).

[19] D. I. Blohincev, V. S. Barašenkov, and V. G. Grišin, Nuovo cimento **9**, 249 (1958).

[19] V. Veksler, Ninth Annual Conference on High-Energy Physics, Kiev, U.S.S.R., 1959 (unpublished).